Smart Structures and Systems, *Vol. 30, No. 6 (2022) 639-648*
https://doi.org/10.12989/sss.2022.30.6.639

Stress evaluation of tubular structures using torsional guided wave mixing

Ching-Tai Ng*[1], Carman Yeung [1a], Tingyuan Yin [1b] and Liujie Chen [2c]

[1] *School of Civil, Environmental & Mining Engineering, The University of Adelaide, Adelaide, 5005 SA, Australia*
[2] *School of Civil Engineering, Guangzhou University, Guangzhou, 510006, China*

(*Received April 19, 2022, Revised August 18, 2022, Accepted October 20, 2022*)

Abstract. This study aims at numerically and experimentally investigating torsional guided wave mixing with weak material nonlinearity under acoustoelastic effect in tubular structures. The acoustoelastic effect on single central frequency guided wave propagation in structures has been well-established. However, the acoustoelastic on guided wave mixing has not been fully explored. This study employs a three-dimensional (3D) finite element (FE) model to simulate the effect of stress on guided wave mixing in tubular structures. The nonlinear strain energy function and theory of incremental deformation are implemented in the 3D FE model to simulate the guided wave mixing with weak material nonlinearity under acoustoelastic effect. Experiments are carried out to measure the nonlinear features, such as combinational harmonics and second harmonics in related to different levels of applied stresses. The experimental results are compared with the 3D FE simulation. The results show that the generation combinational harmonic at sum frequency provides valuable stress information for tubular structures, and also useful for damage diagnosis. The findings of this study provide physical insights into the effect of applied stresses on the combinational harmonic generation due to wave mixing. The results are important for applying the guided wave mixing for in-situ monitoring of structures, which are subjected to different levels of loadings under operational condition.

Keywords: combinational harmonic; guided wave; second harmonic; torsional wave acoustoelastic effect; tubular structure; wave mixing

1. Introduction

Tubular structures have been widely applied as load transferring structures in different engineering disciplines, e.g., civil, mechanical, and offshore engineering structures (Fang *et al*. 2018, Chen *et al*. 2021). When structures are under operational condition, the load carrying members are subjected to repeat tensile and compressive force induced by external applied load, residual, or thermally induced stresses. The effect of stress is unavoidable in structures, and for long-term fatigue may cause structural failure to the loading carrying members. Therefore, it is essential to develop a practical and reliable structural health monitoring (SHM) to assess the condition and ensure the safety of the structures. SHM can be used to provide in-situ integrity monitoring of structure, the understanding of the effect of applied loading on the technique used to monitoring the structures is important. In the literature, different studies were carried out to improve the physical insight and develop techniques for monitoring the stress in structures (Li *et al*. 2019, Hughes *et al*. 2019, Dubuc *et al*. 2020).

To date, different nondestructive evaluation (NDE) and SHM techniques were developed to provide cost effective condition assessment and safety inspection for different engineering structures (Zhang *et al*. 2016, Yin *et al*. 2021, Nasim Khan Raja *et al*. 2021, Allen and Ng 2022). In particular, ultrasonic guided wave has been widely recognized as one of the promising NDE, SHM techniques and/or interrogating the life expectancy of structures. The advantages of the ultrasonic guided wave are long-distance inspection and ability of in-situ online monitoring for inaccessible locations of structures. In the literature, studies on linear guided wave mainly focused on the analysis of wave scattering and mode conversion effect at defect (Cawley and Alleyne 1996, Yeung and Ng 2019). Studies showed that the use of low frequency guided wave (below 250 kHz) is more practical for tubular structures because it minimizes the number of wave modes that can be induced in the low frequency range. Different to linear guided wave, nonlinear guided wave focuses on investigating higher harmonic generation in frequency-domain at early stage of damage (Sohn *et al*. 2014, Pattanayak *et al*. 2015). There were studies focused on higher harmonic generation in cylindrical-like structures. Liu *et al*. (2013) carried out an analytical study. They showed that the secondary harmonic can be generated in longitudinal direction due to shear coupling when the torsional wave is propagating in the cylindrical-like structures.

1.1 Acoustoelastic effect of guided waves

In real applications, the use of ultrasonic guided wave for SHM require to address different technical challenges. For in-situ online SHM, the ultrasonic guided wave data

*Corresponding author, Ph.D., Professor,
E-mail: alex.ng@adelaide.edu.au
[a] Ph.D. Student
[b] Ph.D. Student
[c] Ph.D. Lecturer

ISSN: 1738-1584 (Print), 1738-1991 (Online)

generally is obtained under operational conditions, however, the structures are subjected to various loads in service, which has significant effects on the monitoring data. In the literature, it has been widely reported that the guided wave propagation is affected by the acoustoelastic effect and this effect needs to be considered when the structures are under operational condition. Hence, it is essential to understand and quantify the acoustoelastic effect on guided wave propagation so that the inspection can be carried out reliably and accurately on structures under operational condition.

Different studies have been carried out to understand and quantify the acoustoelastic effect of linear guided wave and their findings and results support the application of ultrasonic guided wave in in-situ online monitoring of structures (Nikitina *et al*. 2009, Kamyshev *et al*. 2010, Liu *et al*. 2013, Bartoli *et al*. 2010, Li *et al*. 2017). From the theoretical aspect, Murnaghan (1937) wrote a book on interpreting finite deformation theory and third order elastic modulus. Latter, Biot (1940) studied the fundamental differences between the stress-free and initially stressed condition, and derived wave equations for wave propagating in pre-stressed media. In the experimental aspect, existing studies focused on measuring linear guided wave features, velocity change, in different structures, e.g., wire strands (Chaki and Bourse 2009) and pipes (Dubuc *et al*. 2017). Hirao *et al*. (1981) investigated the acoustoelastic effect of Rayleigh wave and found out that Rayleigh wave is no longer non-dispersive in the presence of non-uniform stress. Lu *et al*. (1998) carried out a comprehensive study on wave propagation under applied and residual stresses. Some recent works focused on studying the change of the wave speed in the prestressed plate using the theory of incremental deformation (Pau and Lanza di Scalea 2015, Mohabuth *et al*. 2016). From the above studies, they considered the stress effect in the wave propagation and evaluated the change of the wave velocity.

Due to the high sensitivity to micro defects, the number of studies focused on nonlinear guided wave has been increasing recently. Yang *et al*. (2019b) carried out an investigation on the nonlinear features of Lamb wave, such as generation of second harmonic, under acoustoelastic effect in pre-stressed plates. Hughes *et al*. (2019) demonstrated the application of Rayleigh guided wave based on acoustoelasticity, and proposed a new method using second harmonics for stress monitoring. Apart from the second harmonic, the nonlinear technique considering acoustoelasticity and utilizing mixing guided waves also has attracted attention.

2. Mixing of guided waves

In this study, mixing of guided wave refers to the interaction of more than one guided wave with different central frequencies in a structure. Combinational harmonic at the sum and difference of the fundamental excitation frequencies could be generated due to the interaction of the waves. In the literature, the studies of guided wave using single central frequency encountered an obstacle in differentiating material nonlinearity from other unwanted nonlinearity, such as nonlinearities from coupling media and data acquisition system (Yang *et al*. 2019a). Guided wave mixing using two independent physical channels for generating excitation was proposed to overcome this problem as the generated combinational harmonics are not affected by the nonlinear interference from the instruments.

Mixing of guided waves has been studied for different types of structures, such as concrete (McGovern *et al*. 2015) and plate (Hasanian and Lissenden 2017). Pioneer studies have Liu *et al*. (2012), who generated a longitudinal wave and a shear wave in elastic solids and measured the acoustic nonlinear parameter. McGovern *et al*. (2014) studied the nonlinear response of non-collinear bulk wave mixing in concrete. In the literature, research was also carried out on mixing Lamb waves in plates. Hasanian and Lissenden (2018) derived an analytical solution for Lamb wave mixing phenomenon. Li *et al*. (2018) proposed a one-way mixing approach to study the interaction between symmetric and antisymmetric Lamb waves in thin plates. Shan *et al*. (2019) used two shear horizontal waves with collinear interaction approach to interrogate the effect of material nonlinearity in plates. A recent study conducted by Yeung and Ng (2020) experimentally demonstrated the generation of the combinational harmonic at sum and difference frequencies in pipes. Although the literature has shown the benefits of using wave mixing for damage detection, the acoustoelastic effect on guided wave mixing has not been fully investigated. One of the objectives of this paper is to carry out numerical and experimental studies on torsional guided wave mixing in tubular structures under pre-stressed conditions. This paper focuses on understanding the acoustoelastic effect of combination harmonic generation due to wave mixing. In addition, this study also compares the performance of the combination harmonic generation with the second harmonic generation using single central frequency excitation. This study also develops a three-dimensional (3D) finite element (FE) model for predicting the combination harmonic generation due to wave mixing under the acoustoelastic effect. The findings of this study help transfer guided wave mixing techniques to practical in-situ online monitoring.

The paper is organized as follows. The next section first presents the theoretical background of acoustoelasticity with the consideration of material nonlinearity. It then describes the 3D FE model of a tubular structure and the modelling of the loading effect at both ends. The selection of excitation frequencies at low frequency range and the modelling of material nonlinearity are also presented. To demonstrate the sensitivity of the group velocity change in response to the applied stress and differences between linear and nonlinear wave responses, the 3D FE model is used to generate a series of numerical results. The FE predicted acoustoelastic effect of wave mixing is then validated by experimental measurements. The FE simulation and experimental results are used to investigate the acoustoelastic effect on the combinational harmonic and second harmonic generation under different levels of applied stresses. Finally, conclusions are drawn.

3. Nonlinear guided waves under acoustoelastic effect

The theory of generation of second harmonic and combinational harmonic in structures under pre-stressed condition are described in this section. The concept of finite deformation in a structure with weak nonlinear elasticity is used and it is based on continuum mechanics.

3.1 Acoustoelastic effect

Acoustoelastic effect is a nonlinear effect of constitutive relation between mechanical stress and finite strain in an elastic material. The superimposition of incremental motions of a pre-stressed solid on a finite homogeneous deformation can be expressed by a set of governing equations (Ogden 2007). Considering a hyperelastic material in an isotropic medium and defining α_r as free-of-stress configuration (reference) and α_c stressed configuration (current), the Cartesian coordinates $\boldsymbol{X}$ and $\boldsymbol{x}$ are the respective material points at the initial stage and finial stage, respectively. The deformation gradient from α_r to α_c can be expressed by $\mathbf{F} = \mathrm{Grad}\,\boldsymbol{x}$ (Shams *et al.* 2011). The strain energy function W can be related to $\mathbf{F}$ via the principal invariants of the right Cauchy-Green deformation tensor $\mathbf{C} = \mathbf{F}^{\boldsymbol{T}}\mathbf{F}$. The symmetric Cauchy stress tensors can be defined as

$$\boldsymbol{\sigma} = J^{-1}\mathbf{F}\sum_{i=1}^{3} W_i \frac{\partial I_i}{\partial \mathbf{F}} \tag{1}$$

where $I_i, i \in \{1,2,3\}$ are the principal invariants of C and $\boldsymbol{u}(\boldsymbol{x}, t)$ is the displacement of material point x. J^{-1} is the Jacobian determinant, which equals to det($\mathbf{F}$). The incremental governing equation in a pre-stressed structure is

$$A_{0piqj}\frac{\partial^2 u_j}{\partial x_p \partial x_p} = \rho\frac{\partial^2 u_i}{\partial t^2} \tag{2}$$

where ρ is the mass density of the material in α_c. A_{0piqj} is the Eulerian elasticity tensor in the fourth order, where i, j, p, and q $(= 1,2,3)$ represent the Cartesian coordinates.

3.2 Weak material nonlinearity

Material nonlinearity due to the change of microstructures can be used to detect material imperfections. The third-order strain energy function for nonlinear guided waves is defined based on the study of Murnaghan (1937). The nonlinear strain energy function W can be expressed in a power series

$$\begin{aligned} W = {} & \frac{1}{2}(\lambda + 2\mu)i_1^2 - 2mi_1 i_2 - 2\mu i_2 \\ & + \frac{1}{3}(l + 2m)i_1^3 + ni_3 \end{aligned} \tag{3}$$

where l, m and n are the third order elastic constants; λ and μ are the Lamé elastic coefficients. $i_1 = tr\mathbf{E}$, $i_2 = \frac{1}{2}[(tr\mathbf{E})^2 - tr(\mathbf{E})^2]$ and $i_3 = det\mathbf{E}$ are the principal invariants of the Green-Lagrange strain tensor $\mathbf{E}$, which is composed of the Cauchy-Green deformation tensor and the identity tensor $\mathbf{E} = \frac{1}{2}(\mathbf{C} - \mathbf{I})$.

4. Three-dimensional finite element simulation

In this study, a commercial FE software ABAQUS was used to model the wave propagation in a 1m long aluminium tube. The material properties of the aluminium tube are shown in Table 1. The tube has a hollow cross-section with inner radius of 9.5 mm and wall thickness of 3 mm. In ABAQUS the aluminium tube was modelled using C3D8R elements, which is a solid element having three translational degrees-of-freedom at each node. The explicit integration approach was used to solve the dynamic simulation (Yang *et al.* 2018). The mesh size was approximately 0.6 mm × 0.6 mm × 0.6 mm, which ensures the simulation accuracy by having more than 20 nodes exist for the shortest wavelength of the waves considered in this study and five layers of elements across the wall thickness of the tube (Smith 2009). To generate the torsional guided waves, tangential force was applied to eight nodes in circumferential direction, and these nodes were evenly distributed at the circumference of the left end of the tube.

4.1 Frequency selection of torsional guided wave mixing

To avoid the generation of higher order wave modes (Løvstad and Cawley 2011), the low frequency excitation is used in this study. The wave mixing frequencies are f_1 = 70 kHz and f_2 = 110 kHz, which were determined by experimental study to ensure the excited wave signal has large enough amplitude and the harmonic generated due to material nonlinearity in wave mixing is experimentally measurable. In this study, two narrow-band sinusoidal tone burst pulses at f_1 with 15 cycles and f_2 with 10 cycles were first modulated by Hann window individually. They were then added together without time delay to form a combined excitation signal for the wave mixing. Although this frequency combination does not satisfy with the phase matching condition of cumulative effect, this is not the focus in the current study. Since torsional waves do not generate second harmonics torsional waves, the current study focuses on harmonics generation due to the coupling from the fundamental mode of torsional wave T(0,1) to the longitudinal waves. In addition to second harmonic of the individual excitation frequencies, $2f_1$ and $2f_2$, combinational

Table 1 Material properties of aluminum used in the FE simulation

Density (kg/m^3)	ρ	2700
Lamé constants (GPa)	λ	56.68
	μ	27.13
Third order elastic constant (GPa)	l	-277.74
	m	-351.7
	n	-573.94

harmonics at sum and difference frequencies (i.e., $f_2 \pm f_1$) were also induced due to material nonlinearity.

4.2 Finite element modelling of material nonlinearity

The generation of harmonics from torsional guided wave mixing, second harmonics and combinational harmonics are simulated using the constitutive model described in the theoretical section. In this study, ABAQUS/Explicit was used to simulate the wave mixing. A material subroutine VUMAT was implemented to simulate the effect of material nonlinearity. The stress $\hat{\boldsymbol{\sigma}}$ used in ABAQUS subroutine is the Cauchy stress tensor in the basis of Green-Naghdi rate and defined as

$$\hat{\boldsymbol{\sigma}} = \mathbf{R}^{\mathrm{T}}\boldsymbol{\sigma}\mathbf{R} \tag{4}$$

where tensor $\mathbf{R}$ is an orthogonal tensor. The Cauchy stress can be written in terms of second Piola-Kirchhoff stress and the deformation gradient as

$$\hat{\boldsymbol{\sigma}} = \mathrm{J}^{-1}\mathbf{U}\frac{\partial W}{\partial \mathbf{E}}\mathbf{U}^{\mathrm{T}} \tag{5}$$

where $\mathbf{U}$ is the right stretch tensor for local stretching at the position of the material particle in the stress-free reference configuration.

4.3 Pre-loading for simulating pre-stressed condition

To study the acoustoelastic effect in the 3D FE simulation, the quasi-static loading was applied to slowly pre-stress the tubular structure. The quasi-static loading curve as shown in Fig. 1 was gradually increased to minimize the influence on wave generation due to transient effect (Mohabuth *et al*. 2016). In the study, a two-stage approach was used. In Stage 1, the duration of the simulations is 13 ms, in which tensile pressure was first applied on the surface at the two ends of the tubular structure until it reaches a steady state. The tensile pressure is indicated by red arrows in Fig. 2(a). In Stage 2, the mixed T(0,1) wave (f_1 and f_2) was excited at the end of the tubular structure. The yellow arrows shown in Fig. 2(b) indicate the excitation location and direction of the applied loads for generating the incident T(0,1) wave.

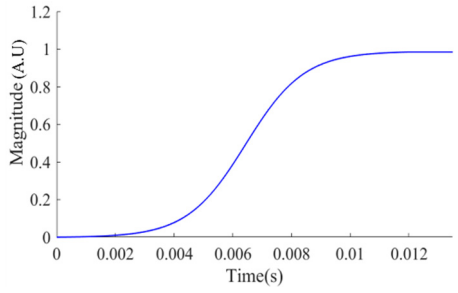

Fig. 1 Quasi-static loading curve for simulating pre-stressed condition

In the FE simulation, the nodes in tangential and longitudinal velocities at 450 mm away from the excitation location were calculated. Different magnitudes of stresses from 0 MPa to 80 MPa in steps of 20 MPa were considered in this study to have a better understanding of the stress effect on wave propagation in tubular structures. In the simulation, the stress-strain condition is below elastic limit in all five cases.

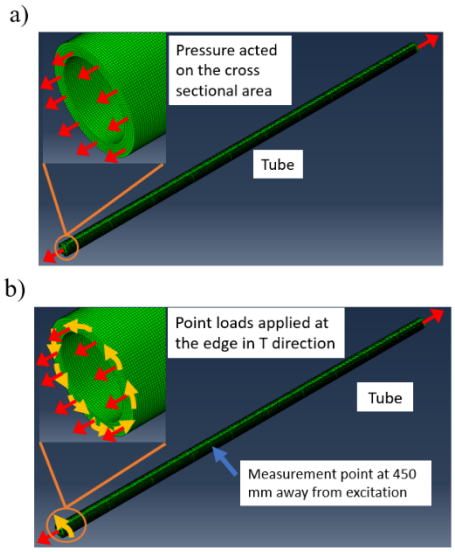

Fig. 2 Schematic diagram of the two-stage approach: a) applied tensile pressure at both ends of the tubular structure in Stage 1; and b) excitation for generating torsional wave in Stage 2

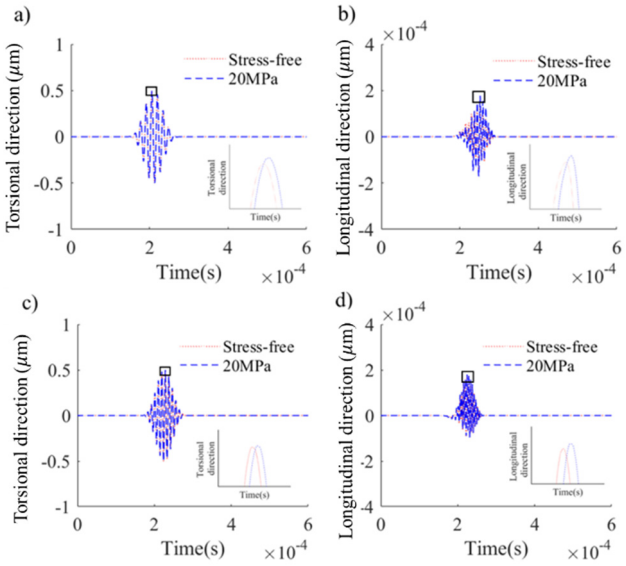

Fig. 3 FE simulated wave propagation at stress-free and 20 MPa in torsional direction and longitudinal direction at a) & b) f_1 and c) & d) f_2 with nonlinear material properties

4.4 Change of group velocity in pre-stressed tubular structure

The group velocity of guided wave is the velocity with the overall envelope shape propagate through the medium. The change of group velocity can be used as an indicator of the pre-stress level in structures. In this study, a comparison of wave velocity measured in torsional and longitudinal directions under stress-free and pre-stressed states at 20 MPa is shown in Fig. 3. A shift is observed at the peaks in both torsional and longitudinal directions when a tensile pressure of 20 MPa is applied at the end of the tubular structure. The results of the reference FE simulations using linear material properties is shown in Fig. 4, in which the peak of the guided wave signal is not shifted for the tubular structure under stress-free and pre-stressed state. It should be noted that the time domain signal in longitudinal direction has distortion in the nonlinear response as shown in Figs. 3(b) and 3(d). But this is not visible in linear response as shown in Figs. 4(b) and 4(d). Similar phenomenon of the distorted response was found in (Shan *et al*. 2019). It is believed that material nonlinearity associated with self-interaction is possibly the cause of the distortion. The primary harmonics at f_1 and f_2 in the longitudinal motion are also generated due to the non-planar wavefront generated by finite width excitation points (Deng *et al*. 2017). The magnitude of the longitudinal motion for nonlinear signal induced by the material nonlinearity is approximately ten times larger than that for linear signal.

Fig 5 shows a further analysis of the acoustoelastic effect in tubular structures. As the nonlinear material behavior with acoustoelastic effect distributes along the tube, the group velocities are obtained by averaging the velocities calculated at five consecutive measurement points. The results show that both torsional and longitudinal waves at frequencies f_1 (Fig. 5(a)) and f_2 (Fig. 5(b)) have a similar decreasing trend in the group velocity changes for the five levels of stresses considered in this study. But the group velocity changes of the torsional and longitudinal waves are different. The results confirm that the group velocity change due to acoustoelastic effect is not significant.

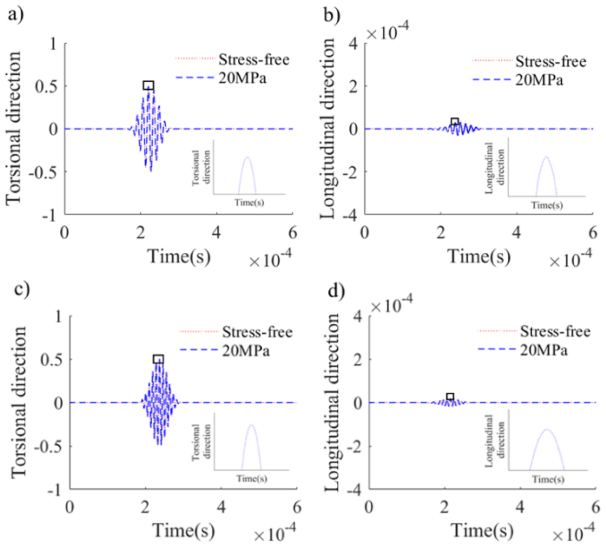

Fig. 4 FE simulated wave propagation at stress-free and 20 MPa in torsional direction and longitudinal direction at a) & b) f_1 and c) & d) f_2 with linear material properties

4.5 Comparison of linear and nonlinear guided waves

Time-frequency spectra of the simulated signals using Short Time Fourier Transform (STFT) is shown in Fig. 6. A mixed frequency signal (f_1 and f_2) was used as the excitation and the tubular structure was subjected to a tensile pressure of 20 MPa to study the linear and nonlinear guided wave signals. Fig. 6(d) shows the nonlinear wave induced due to microstructural changes in a material. From the results it shows that the harmonics, such as second harmonics ($2f_1$ and $2f_2$), and combinational harmonics at sum and difference frequencies (f_2+f_1 and f_2-f_1), are observed in the nonlinear longitudinal wave signals. But only the primary wave modes (f_1 and f_2) are observed in the linear signals. The results shown in Fig. 6 are similar to the results from the findings from the previous study (Yeung and Ng 2020). There is no other harmonics in the linear torsional wave as shown in Fig. 6(a) and 6(c)) with or without the use of nonlinear strain energy function, and only the fundamental frequencies at f_1 and f_2 are observed. Fig. 6(d) shows that the generation of second and combinational harmonics at frequencies $2f_1$, $2f_2$, f_2+f_1 and f_2-f_1 are observed in the longitudinal direction due to the shear coupling phenomenon and the material nonlinearity. Furthermore, the time-frequency representation (TFR) dispersion curve for the first two longitudinal modes L(0,1) and L(0,2) and first torsional mode T(0,1) were also depicts together with time-frequency spectra in Fig. 6(d). It is observed that the combinational harmonic at sum frequency is longitudinal wave mode L(0,2) while the second harmonic frequency at $2f_1$ is the longitudinal wave mode L(0,1).

In the numerical simulation of guided wave mixing in tubular structures, it allows separating the time-domain

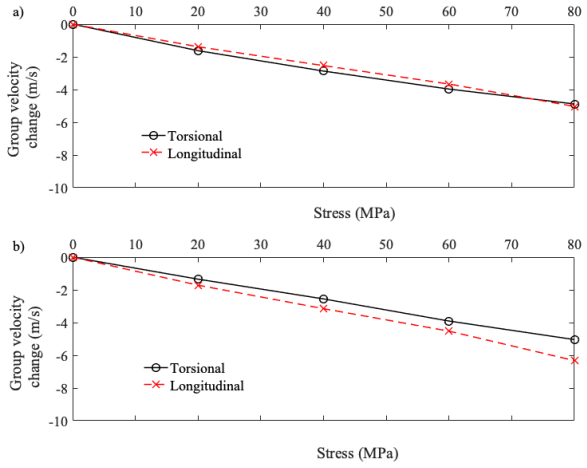

Fig. 5 Change of group velocity due to different levels of pre-stress at frequencies (a) f_1 and (b) f_2

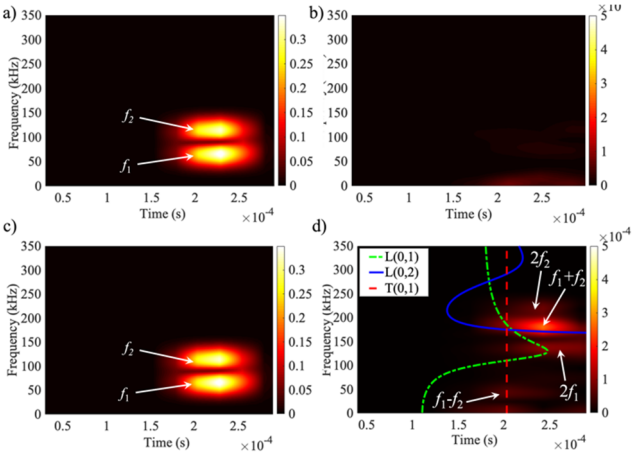

Fig. 6 Time-frequency spectra of (a) linear torsional; (b) linear longitudinal; (c) nonlinear torsional; and (d) nonlinear longitudinal waves

signal into torsional and longitudinal directions to gain better understanding in the generation of combinational harmonics. Fig. 7 is the frequency spectra of the time-domain signals obtained by Fast Fourier Transform (FFT), in which Fig. 7(a) is the signal in the torsional direction while Fig. 7(b) is in the longitudinal direction. The frequencies of excitation, second harmonics and combinational harmonics are indicated by vertical dotted lines. The red dash-dot line is presented in Fig. 7(b). It represents linear guided wave signal, which only has peaks at excitation frequencies f_1 and f_2. The blue dashed line indicates the nonlinear guided wave response and it has the second harmonics ($2f_1$ and $2f_2$) and combinational harmonics (f_2-f_1 and f_2+f_1). It should be noted that the

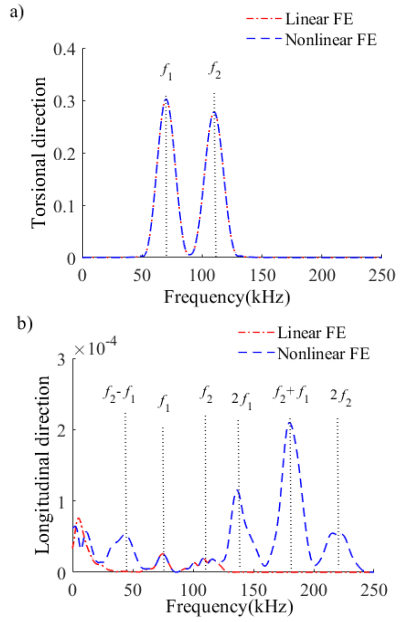

Fig. 7 FE simulated frequency-domain signals at the mixed frequency (f_1 and f_2) subjected to 20MPa tensile stress in (a) torsional; and (b) longitudinal direction

generation of f_1 and f_2 components in the longitudinal direction is due to non-planar wavefront generated by finite width excitation points (Deng *et al*. 2017).

5. Experimental validation

5.1 Experimental setup

The specimen used in the experiment is a 1 m long aluminium tube and it has the same dimension as the FE model described in Section 4. To generate the wave, four 6 mm × 6 mm × 1 mm piezoceramic shear transducers were bonded on the surface of the tube using conductive epoxy adhesive. Although there is a small gap between both ends of the transducer and the curved pipe surface, the gap is relatively small given the length of the transducer is small, and the gap was filled by the conductive epoxy adhesive. Fig. 8 shows a schematic diagram of the experimental setup. The tube was attached to the MTS load testing machine (Model 45) and the pre-stressed loading was applied before the wave signal collection. A mixed frequency signal at f_1 and f_2 with the same number of cycles as in the FE simulations was first created by a computer-controlled function generator (NI PIX-5412). The use of the low frequency excitation is to prevent the generation of high-order wave modes. The signal was amplified by KROHN-HITE 7500 before it was sent to the actuator. The guided wave signal was measured by the other shear transducer, but it was rotated so that the polarization direction of the receiving shear transducer is perpendicular to the actuation direction of the shear transducer. This maximizes the measurement in the longitudinal direction. The location of the receiving shear transducer was located 450 mm away from the excitation location. The received signals were digitized by NI PIXe-5105. The signals were averaged 500 times and sampling rate is 100 MHz.

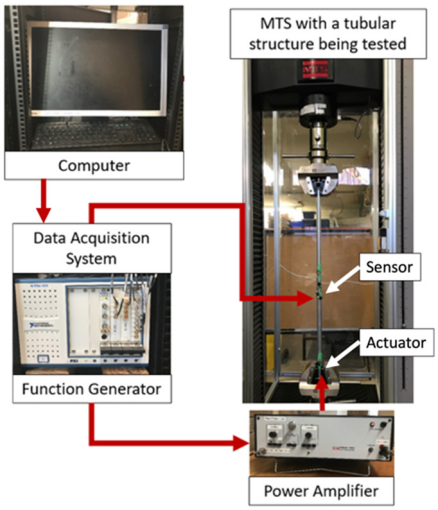

Fig. 8 Experimental setup for guided wave mixing with acoustoelastic effect

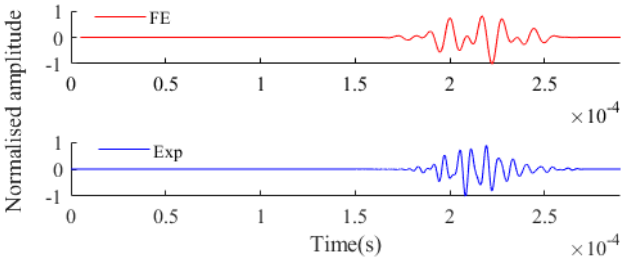

Fig. 9 Comparison of time-domain signals between FE (top) and experiment (bottom)

5.2 Validation of harmonics generation

The mixed frequency signals in both torsional and longitudinal directions were measured by the transducer. Furthermore, for better comparison of time-domain results at a notionally common scale, both experimental and FE data were normalized through divided by the maximum value of their own group. Hence, the maximum data points should be one and other points were scaled equally. Fig. 9 shows the normalized experimental data (blue line) and the FE simulated result (red line). The wave signals in the FE model and the experiment have the same arrival time.

Fig. 10 compares the signals between the experimentally measured data and the FE simulated data. The data was transferred to time-frequency domain by STFT and extracted at the combinational harmonics at sum and difference frequencies (f_1-f_2 and f_1+f_2), and second harmonic frequencies ($2f_1$ and $2f_2$). The experimentally measured and FE simulated signals have a consistent decreasing trend, and the amplitude of the sum of combinational harmonic $f_1 + f_2$ is larger than other harmonics. The results in the figure show a good agreement between FE simulated and experimentally measured data.

Fig. 11 compares the second harmonic frequencies at $2f_1$ and $2f_2$ for mixed and single frequency excitation signal in

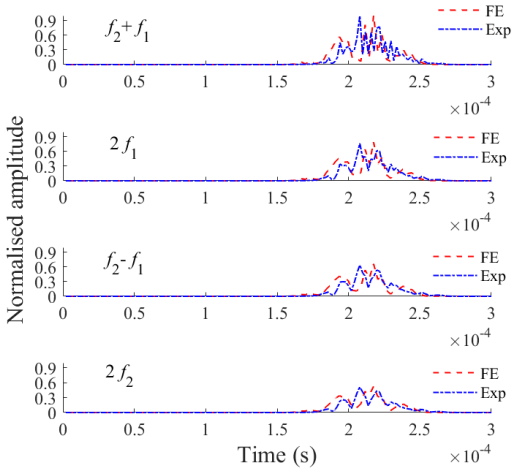

Fig. 10 Comparison of experimentally measured and FE simulated data extracted at the combinational harmonics at sum and difference frequencies (f_1–f_2 and f_1+f_2), and second harmonic frequencies ($2f_1$ and $2f_2$)

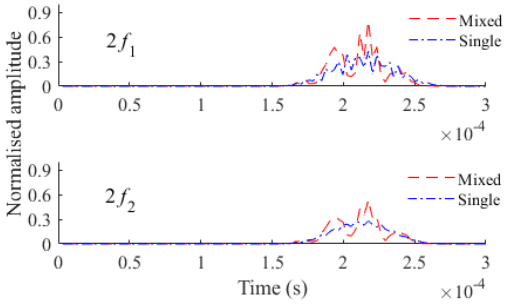

Fig. 11 FE simulated data extracted at second harmonic frequency for excitation signal using mixed frequency and single frequency

longitudinal direction. They are the FE simulated results and extracted at the second harmonic frequency using STFT. It should be noted that the signals of mixed frequency have larger amplitude than that of single frequency excitation signals.

6. Application of combinational and second harmonic of wave mixing for stress monitoring

The acoustoelastic effect on guided wave mixing in tubular structures has been validated in the experimental validation section. As shown in Section 5, second and combinational harmonics can only be induced in the longitudinal direction. This section investigates the feasibility of using of combinational harmonic and second harmonic of wave mixing on monitoring the stress in tubular structures, and exams the performance of these harmonic for stress monitoring. To monitor the stress in tubular structures, nonlinear parameters $\beta'_{comb,mix}$ and $\beta'_{2nd,mix}$ are defined to quantify the generation of combinational and second harmonics in guided wave mixing (Croxford *et al*. 2009). The nonlinear parameters are defined as

$$\beta'_{comb,mix} = \frac{A_{f_1 \pm f_2}}{A_{f_1} A_{f_2}} \tag{6}$$

$$\beta'_{2nd,mix} = \frac{A_{2,mix}}{A^2_{1,mix}} \tag{7}$$

where $A_{f_1 \pm f_2}$, A_{f_1}, A_{f_2}, $A_{2,mix}$ and $A_{1,mix}$ are the amplitude of the combinational harmonics at sum and difference frequencies, the amplitude of primary frequencies at f_1 and f_2, the amplitude of second harmonics and the corresponding amplitude of the fundamental harmonic, respectively.

The experimentally measured and FE simulated results of the harmonics under different magnitudes of tensile stresses are shown in Fig. 12. The nonlinear parameters of FE simulation were normalized by dividing the nonlinear parameter of sum frequency $(f_1 + f_2)$ at 0 MPa. The experimental nonlinear parameters were normalized in the same way. Good agreement is obtained in the trend of the experimentally measured and FE simulated results. The

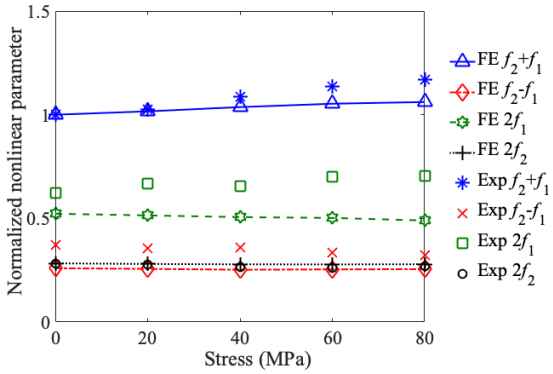

Fig. 12 Nonlinear parameters of responses in longitudinal direction with different levels of stress

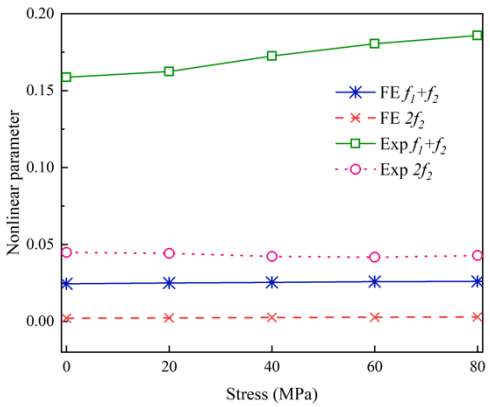

Fig. 13 Nonlinear parameters of the combinational harmonic at sum frequency using wave mixing and second harmonic using single frequency excitation

results show that the combinational harmonic at sum frequency has the largest value for all stress levels. The amplitude of the sum frequency increases from stress-free state to pre-stressed state at 80 MPa in a step of 20 MPa. Meanwhile, the amplitude at $2f_1$ slightly decreases and the amplitudes at $2f_2$ and $f_2 - f_1$ remain constant from 0 MPa to 80 MPa. The results confirmed that the sum frequency component belongs to L(0,2) mode of wave as shown in Fig. 6(d), which is based on the traveling time of the wave at sum frequency. The dominance of this frequency component can be explained by the modeshape of L(0,2) as it has a larger magnitude than L(0,1). Also, L(0,1), and L(0,2) waves have similar arrival time. The results show that the combinational harmonic at sum frequency is more sensitive to the acoustoelastic effect, especially when the tube is subjected stresses.

Fig. 13 presents the other numerical and experimental study that compares the combinational harmonic at sum frequency in wave mixing approach and the second harmonic using single frequency excitation signal. The single frequency excitation is one of the primary frequencies at f_2 used in this study, and they are the same for the five pre-stressed cases. This study aims at observing the trend of the nonlinear parameters between the mixed frequency and single frequency excitation signal. A nonlinear parameter $\beta'_{2nd,single}$ for single frequency is defined as (Croxford *et al*. 2009)

$$\beta'_{2nd,single} = \frac{A_{2,single}}{A_1^2} \tag{8}$$

where A_1 and $A_{2,single}$ are the magnitude of the incident frequency and the corresponding second harmonic, respectively.

Fig. 13 compares the frequency response of FE simulation and experiments at $f_1 + f_2$ induced by guided wave mixing with the frequency response at $2f_2$ induced by the single frequency. The combinational harmonic at sum frequency (i.e., $f_1 + f_2$) shows an ascending trend and the magnitude is larger than the second harmonic using single frequency excitation. For the case of the single frequency excitation of the FE simulation, the nonlinear parameter ($\beta'_{2nd,single}$) of second harmonic ($2f_2$) is purely generated from the single frequency excitation due to the material nonlinearity and has an increasing trend. For the FE wave mixing case, the magnitude of the combinational harmonic at sum frequency ($\beta'_{comb,mix}$) also has an increasing trend and the amplitude is approximately ten times larger than the amplitude of the second harmonic generated from single frequency excitation. Additionally, in the experimental results, the nonlinear parameters ($\beta'_{comb,mix}$) at various stress states are generally three times larger compared to the nonlinear parameter ($\beta'_{2nd,single}$). This indicates that the combinational harmonic is easier to be measured reliably so it is a better option for monitoring the stress level of tubular structures in real applications.

7. Conclusions

This study has investigated the acoustoelastic effect on torsional guided wave mixing and demonstrated the use of combinational harmonic at sum frequency to monitor the stress in tubular structures. The study has focused on understanding and quantifying the acoustoelastic effect on the combinational harmonic generation due to material nonlinearity. 3D FE simulations and experiments considered different level of stresses applied on the tubular structures have been carried. The 3D FE model has used the nonlinear strain energy function to consider the material nonlinearity and the acoustoelastic effect of the guided wave mixing. The 3D FE model has been validated by the experiment data in predicting the combinational harmonic and second harmonic generation due to wave mixing and subjected to acoustoelastic effect. Good agreement between FE and experimental data has been observed.

This study has also presented a series of case studies numerically and experimentally to investigate the acoustoelastic effect on the combinational harmonic and second harmonic generated from wave mixing. The results have shown that the magnitude of the generated combinational harmonic at sum frequency has greater amplitude and better sensitive to the acoustoelastic effect compared to the combinational harmonic at difference frequency and second harmonics. The results have shown that the combinational harmonic at sum frequency is a

better choice for monitoring the stress of tubular structures. The study has also compared the generation of combinational harmonic at sum frequency using wave mixing with second harmonic using single excitation frequency. The results show that the combinational harmonic at sum frequency using wave mixing has much greater magnitude compared to the second harmonic using single frequency, which is expected to have better performance for monitoring the stress in tubular structures.

The findings of this study not only improve the understanding of the influence of stress on nonlinear measurements, but also support the application of wave mixing in in-situ online monitoring of structures. It is important to understand the acoustoelastic effect of nonlinear guided wave mixing because structures are usually subjected to different loading under operational condition. Therefore, the findings of this study have ensured the nonlinear guided wave mixing approach can be used reliably and accurately in the in-situ online monitoring of tubular structures.

Acknowledgments

This work was supported by the Australian Research Council through DP200102300 and DP210103307. The support is greatly appreciated.

References

Allen, J.C.P. and Ng, C.T. (2022), "Debonding detection at adhesive joints using nonlinear Lamb waves mixing", *NDT & E Int*., **125**, 102552. https://doi.org/10.1016/j.ndteint.2021.102552

Bartoli, I., Phillips, R., Coccia, S., Srivastava, A., di Scalea, F.L., Fateh, M. and Carr, G. (2010), "Stress dependence of ultrasonic guided waves in rails", *Transp. Res. Rec*., **2159**(1), 91-97. https://doi.org/10.3141/2159-12

Biot, M.A. (1940), "The influence of initial stress on elastic waves", *J. Appl. Phys*., **11**(8), 522-530. https://doi.org/10.1063/1.1712807

Cawley, P. and Alleyne, D. (1996), "The use of Lamb waves for the long range inspection of large structures", *Ultrasonics*, **34**(2-5), 287-290. https://doi.org/10.1016/0041-624x(96)00024-8

Chaki, S. and Bourse, G. (2009), "Stress level measurement in prestressed steel strands using acoustoelastic effect", *Exp. Mech*., **49**(5), 673-681. https://doi.org/10.1007/s11340-008-9174-9

Chen, J., Fang, H. and Chan, T.-M. (2021), "Design of fixed-ended octagonal shaped steel hollow sections in compression", *Eng. Struct*., **228**, 111520. https://doi.org/10.1016/j.engstruct.2020.111520

Croxford, A.J., Wilcox, P.D., Drinkwater, B.W. and Nagy, P.B. (2009), "The use of non-collinear mixing for nonlinear ultrasonic detection of plasticity and fatigue", *J. Acoust. Soc. Am*., **126**(5), EL117-EL122. https://doi.org/10.1121/1.3231451

Deng, M., Gao, G., Xiang, Y. and Li, M. (2017), "Assessment of accumulated damage in circular tubes using nonlinear circumferential guided wave approach: a feasibility study", *Ultrasonics*, **75**, 209-215. https://doi.org/10.1016/j.ultras.2016.12.001

Dubuc, B., Ebrahimkhanlou, A. and Salamone, S. (2017), "Effect of pressurization on helical guided wave energy velocity in fluid-filled pipes", *Ultrasonics*, **75**, 145-154. https://doi.org/10.1016/j.ultras.2016.11.013

Dubuc, B., Ebrahimkhanlou, A. and Salamone, S. (2020), "Stress monitoring of prestressing strands in corrosive environments using modulated higher-order guided ultrasonic waves", *Struct. Health Monit*., **19**(1), 202-214. https://doi.org/10.1177/1475921719842385

Fang, H., Chan, T.-M. and Young, B. (2018), "Structural performance of cold-formed high strength steel tubular columns", *Eng. Struct*., **177**, 473-488. https://doi.org/10.1016/j.engstruct.2018.09.082

Hasanian, M. and Lissenden, C.J. (2017), "Second order harmonic guided wave mutual interactions in plate: Vector analysis, numerical simulation, and experimental results", *J. Appl. Phys*., **122**(8), 084901. https://doi.org/10.1063/1.4993924

Hasanian, M. and Lissenden, C.J. (2018), "Second order ultrasonic guided wave mutual interactions in plate: Arbitrary angles, internal resonance, and finite interaction region", *J. Appl. Phys*., **124**(16), 164904. https://doi.org/10.1063/1.5048227

Hirao, M., Fukuoka, H. and Hori, K. (1981), "Acoustoelastic effect of Rayleigh surface wave in isotropic material", *J. Appl. Mech.-Transact. ASME*, **48**(1), 119-124. https://doi.org/10.1115/1.3157553

Hughes, J.M., Vidler, J., Ng, C.-T., Khanna, A., Mohabuth, M., Rose, L.F. and Kotousov, A. (2019), "Comparative evaluation of in situ stress monitoring with Rayleigh waves", *Struct. Health Monit*., **18**(1), 205-215. https://doi.org/10.1177/1475921718798146

Kamyshev, A., Nikitina, N. and Smirnov, V. (2010), "Measurement of the residual stresses in the treads of railway wheels by the acoustoelasticity method", *Russ. J. Nondestruct. Test*., **46**(3), 189-193. https://doi.org/10.1134/S106183091003006x

Li, G.-Y., He, Q., Mangan, R., Xu, G., Mo, C., Luo, J., Destrade, M. and Cao, Y. (2017), "Guided waves in pre-stressed hyperelastic plates and tubes: Application to the ultrasound elastography of thin-walled soft materials", *J. Mech. Phys. Solids*, **102**, 67-79. https://doi.org/10.1016/j.jmps.2017.02.008

Li, F., Zhao, Y., Cao, P. and Hu, N. (2018), "Mixing of ultrasonic Lamb waves in thin plates with quadratic nonlinearity", *Ultrasonics*, **87**, 33-43. https://doi.org/10.1016/j.ultras.2018.02.005

Li, Z., He, J., Teng, J., Huang, Q. and Wang, Y. (2019), "Absolute stress measurement of structural steel members with ultrasonic shear-wave spectral analysis method", *Struct. Health Monit*., **18**(1), 216-231. https://doi.org/10.1177/1475921717746952

Liu, M., Tang, G., Jacobs, L.J. and Qu, J. (2012), "Measuring acoustic nonlinearity parameter using collinear wave mixing", *J. Appl. Phys*., **112**(2), 024908. https://doi.org/10.1063/1.4739746

Liu, Y., Khajeh, E., Lissenden, C.J. and Rose, J.L. (2013), "Interaction of torsional and longitudinal guided waves in weakly nonlinear circular cylinders", *J. Acoust. Soc. Am*., **133**(5), 2541-2553. https://doi.org/10.1121/1.4795806

Løvstad, A. and Cawley, P. (2011), "The reflection of the fundamental torsional guided wave from multiple circular holes in pipes", *NDT & E Int*., **44**(7), 553-562. https://doi.org/10.1016/j.ndteint.2011.05.010

Lu, W., Peng, L. and Holland, S. (1998), *Measurement of acoustoelastic effect of Rayleigh surface waves using laser ultrasonics in Review of Progress in Quantitative Nonestructive Evaluation*, Springer, pp. 1643-1648.

McGovern, M., Buttlar, W. and Reis, H. (2014), "Characterisation of oxidative ageing in asphalt concrete using a non-collinear ultrasonic wave mixing approach", *Insight: Non-Destr. Test. Cond. Monit*., **56**(7), 367-374. https://doi.org/10.1784/insi.2014.56.7.367

McGovern, M., Buttlar, W. and Reis, H. (2015), "Estimation of oxidative ageing in asphalt concrete pavements using non-

collinear wave mixing of critically-refracted longitudinal waves", *Insight*: *Non-Destr*. *Test*. *Cond*. *Monit*., **57**(1), 25-34. https://doi.org/10.1784/insi.2014.57.1.25

Mohabuth, M., Kotousov, A. and Ng, C.-T. (2016), "Effect of uniaxial stress on the propagation of higher-order Lamb wave modes", *Int*. *J*. *Non-Linear Mech*., **86**, 104-111. https://doi.org/10.1016/j.ijnonlinmec.2016.08.006

Murnaghan, F.D. (1937), "Finite deformations of an elastic solid", *Am*. *J*. *Math*., 59(2), 235-260. https://doi.org/10.2307/2371405

Nasim Khan Raja, B., Miramini, S., Duffield, C., Chen, S. and Zhang, L. (2021), "A Simplified Methodology for Condition Assessment of Bridge Bearings Using Vibration Based Structural Health Monitoring Techniques", *Int*. *J*. *Struct*. *Stabil*. *Dyn*., **21**(10), 2150133. https://doi.org/https://doi.org/10.1142/S0219455421501339

Nikitina, N.Y., Kamyshev, A. and Kazachek, S. (2009), "Application of the acoustoelasticity phenomenon in studying stress states in technological pipelines", *Russ*. *J*. *Nondestruct*. *Test*., **45**(12), 861-866. https://doi.org/10.1134/S1061830909120043

Ogden, R.W. (2007), *Incremental statics and dynamics of pre-stressed elastic materials in Waves in nonlinear pre-stressed materials*, Springer, pp. 1-26.

Pattanayak, R.K., Manogharan, P., Balasubramaniam, K. and Rajagopal, P. (2015), "Low frequency axisymmetric longitudinal guided waves in eccentric annular cylinders", *J*. *Acoust*. *Soc*. *Am*., **137**(6), 3253-3262. https://doi.org/10.1121/1.4921269

Pau, A. and Lanza di Scalea, F. (2015), "Nonlinear guided wave propagation in prestressed plates", *J*. *Acoust*. *Soc*. *Am*., **137**(3), 1529-1540. https://doi.org/10.1121/1.4908237

Shams, M., Destrade, M. and Ogden, R.W. (2011), "Initial stresses in elastic solids: constitutive laws and acoustoelasticity", *Wave Motion*, **48**(7), 552-567. https://doi.org/10.1016/j.wavemoti.2011.04.004

Shan, S., Hasanian, M., Cho, H., Lissenden, C.J. and Cheng, L. (2019), "New nonlinear ultrasonic method for material characterization: Codirectional shear horizontal guided wave mixing in plate", *Ultrasonics*, **96**, 64-74. https://doi.org/10.1016/j.ultras.2019.04.001

Smith, M. (2009), ABAQUS/Standard User's Manual, Version 6.9. [available online]

Sohn, H., Lim, H.J., DeSimio, M.P., Brown, K. and Derriso, M. (2014), "Nonlinear ultrasonic wave modulation for online fatigue crack detection", *J*. *Sound Vib*., **333**(5), 1473-1484. https://doi.org/10.1016/j.jsv.2013.10.032

Yang, Y., Ng, C.-T. and Kotousov, A. (2018), "Influence of crack opening and incident wave angle on second harmonic generation of Lamb waves", *Smart Mater*. *Struct*., **27**(5), 055013. https://doi.org/10.1088/1361-665X/aab867

Yang, Y., Ng, C.-T. and Kotousov, A. (2019a), "Second-order harmonic generation of Lamb wave in prestressed plates", *J*. *Sound Vib*., **460**, 114903. https://doi.org/10.1016/j.jsv.2019.114903

Yang, Y., Ng, C.T., Mohabuth, M. and Kotousov, A. (2019b), "Finite element prediction of acoustoelastic effect associated with Lamb wave propagation in pre-stressed plates", *Smart Mater*. *Struct*., **28**(9), 095007. https://doi.org/10.1088/1361-665X/ab2dd3

Yeung, C. and Ng, C.T. (2019), "Time-domain spectral finite element method for analysis of torsional guided waves scattering and mode conversion by cracks in pipes", *Mech*. *Syst*. *Signal Process*., **128**, 305-317. https://doi.org/10.1016/j.ymssp.2019.04.013

Yeung, C. and Ng, C.T. (2020), "Nonlinear guided wave mixing in pipes for detection of material nonlinearity", *J*. *Sound Vib*., **485**, 115541. https://doi.org/10.1016/j.jsv.2020.115541

Yin, T., Ng, C.-T. and Kotousov, A. (2021), "Damage detection of ultra-high-performance fibre-reinforced concrete using a harmonic wave modulation technique", *Constr*. *Build*. *Mater*., **313**, 125306. https://doi.org/10.1016/j.conbuildmat.2021.125306

Zhang, L.H., Maizuar, M., Mendis, P., Duffield, C. and Thompson, R. (2016), "Monitoring the dynamic behaviour of concrete bridges using non-contact sensors (IBIS-S)", *Appl*. *Mech*. *Mater*., **846**, 225-230. https://doi.org/10.4028/www.scientific.net/AMM.846.225